Journal of Alloys and Compounds 509 (2011) 241–245

Contents lists available at ScienceDirect

Journal of Alloys and Compounds

journal homepage: www.elsevier.com/locate/jallcom

The compositions of metastable phase precipitates observed at peak hardness condition in an Al–Mg–Si alloy

S.K. Son[a,1], S. Matsumura[a], K. Fukui[b], M. Takeda[b,*]

[a] Research Laboratory for High-Voltage Electron Microscope, Kyushu University, Hakozaki 6-10-1, Higashi-ku, Fukuoka 812-8581, Japan
[b] Department of Materials Engineering (SEISAN), Yokohama National University, 79-5 Tokiwadai, Hodogaya-ku, Yokohama, 240-8501, Japan

ARTICLE INFO

Article history:
Received 16 June 2010
Received in revised form 12 August 2010
Accepted 25 August 2010
Available online 9 September 2010

Keywords:
Al–Mg–Si
Precipitation behavior
Metastable phase precipitates
Atomic composition
TEM-EDX

ABSTRACT

The metastable-phase precipitates which appear at the peak condition of hardness in an Al–0.83 at%Mg–0.4 at%Si alloy were investigated, using a combination of Vickers microhardness tests, DSC calorimetry, and field-emission STEM observations with EDX analyses. EDX and elemental mapping revealed that both Si-rich and Mg–Si precipitates with needle-shapes were present. EDX analysis showed that needle-shaped β″precipitates protruding from the specimen foils were composed mainly of Si. The present results on structures, compositions and thermal stabilities of the precipitates suggest that Si-rich precipitates co-exist with complex Mg–Si precipitates also of needle-shape.

1. Introduction

Al–Mg–Si ternary alloys are perhaps the most important precipitation-hardening Al-base alloys. This class of alloys is produced in the largest quantity among Al-base alloys, and currently is used widely in construction and transportation applications, because of their superb strength and high-corrosion resistance attained with a combination of conventional components: Al, Mg and Si. In such alloys, the composition and processing conditions to achieve the best properties should be properly chosen, since both the composition and the stage of precipitation influence significantly the properties of the alloys. Hence, numerous studies have been devoted to elucidate the aging sequence and metastable phases which are supposed to be responsible for controlling the mechanical properties.

Most early studies of Al–Mg–Si ternary alloys were based on an assumption that the phase decomposition of supersaturated alloys occurs in the pseudo-binary Al–Mg_2Si alloy system, and accordingly it was believed that metastable precipitates comprise Mg and Si atoms in a ratio of Mg:Si = 2:1. It was reported that the precipitation sequence is solute clusters → metastable β″ precipitates → metastable β′ precipitates → stable βprecipitates [1–3]. Most successive studies followed this interpretation until the 1980s and even later. However, several investigators in the 1980–1990s presented different results and interpretations [4–10]. Lynch et al. were the first to apply field-emission transmission electron microscopy (FE-TEM) to investigate the precipitation processes occurring in an Al–1.16Mg_2Si alloy [4]. They found that the composition of the β″phase was $Mg_{0.44}Si$. In a similar study by FE-TEM and EDX, Edwards et al. [5] reported that needle-shaped β″phase precipitates appearing at the peak hardness condition in an alloy with excess Si content had a Mg:Si ratio nearly equal to 1:1. Three-dimensional atom probe (3DAP) analyses performed by Murayama and Hono [6] also suggested that the atomic ratio of Mg:Si in β″precipitates was close to 1:1. Takeda at al. examined precipitation sequences in Al–Mg–Si alloy specimens with various compositions, using DSC measurements, Vickers microhardness tests and TEM, and concluded that the β″precipitates which formed during isothermal aging at 433–513 K were Si-rich [7,8]. Zandbergen and coworkers claimed that the composition of the β″precipitates is Mg_5Si_6 and the precipitates are fine needles. These authors used HRTEM including the newest image reconstruction technique as well as theoretical simulations based on density functional theory and concluded that the crystal structure was based on a C-centered monoclinic lattice [9,10]. Ramachandran et al. also obtained a similar result using HRTEM and electron diffraction [11]. On the other hand, Matsuda et al. [12] proposed a structure model with a monoclinic lattice and a chemical composition of Si:Al:Mg = 6:3:1 for the needle-shaped β″precipitates in a 0.4 at% excess Si Al–Mg–Si alloy. Fukui et al. made systematic DSC measurements to examine the evolution of metastable phase par-

* Corresponding author.
E-mail address: t1k4d1@ynu.ac.jp (M. Takeda).
[1] Present address: Highnics Electric Co.

0925-8388/$ – see front matter © 2010 Elsevier B.V. All rights reserved.
doi:10.1016/j.jallcom.2010.08.151

ticles and suggested that three metastable reactions occur during the formation of β″precipitates [13–15]. Thus, despite a fairly large number of investigations in the last two decades, an understanding of the microstructure and composition of metastable precipitates appearing at the peak condition of hardness has not completely been established and is still argued.

Concerning the shapes of β″precipitates, electron tomography is a very powerful means of providing three-dimensional (3-D) information on the precipitate morphology [16,17]. We have partly reported an investigation on the 3-D morphology of the precipitates previously [18]. The main results obtained in our study may be summarized thus: only needle-shaped precipitates lying in the crystallographic ⟨1 0 0⟩ directions of the Al matrix were observed at the peak-aging condition, and some of these needle-shaped precipitates were perpendicular to the specimen surfaces. Although the former result is consistent with previous studies, it does not completely exclude the possibility that precipitates with similar shapes have different natures.

The present study aims at elucidating the shapes and compositions of the precipitates in an Al–0.83%Mg–0.4Si (at%) alloy with an approximate balanced composition (Mg:Si= 2:1). We have used a combination of FE-TEM, STEM, energy-dispersive X-ray spectroscopy (EDX) and elemental-mapping techniques which attain a high efficiency and precision in local element-analysis. We have complemented these techniques with Vickers hardness tests and DSC measurements. Since the metastable precipitates which are formed at the peak condition of hardness are the targets of the present study, the TEM work was concentrated on the precipitates which appeared at the peak condition.

2. Experimental

An Al–0.83Mg–0.4Si (at%) alloy ingot with a balanced composition (Mg:Si= ~2:1, in atomic ratio) was used in this study. All specimens for the present experiments were solution-treated at 828 K for 3.6 ks, followed by quenching in ice water. Artificial aging was carried out successively at 483 K in an oil-bath, for various periods up to 60 ks. The Vickers microhardness tests were conducted using a Shimadzu HMV-2000 tester with a 0.98N load. Differential scanning calorimetric (DSC) measurements were carried out with the specimens aged at 483 K for 0–1.2 × 10^5 s, using a RIGAKU TAS300-8230D apparatus. Thin-foil specimens for TEM observations were prepared by electro-polishing in a solution comprising methanol and 25 vol.% nitric acid, using a Struers TENUPOL-5 jet polisher. The STEM-EDX experiments were performed with a nano-probe electron beam approximately 1 nm in diameter, using an FEI Tecnai 20 STEM operated at 200 kV.

3. Results and discussion

3.1. Vickers microhardness and DSC measurements

The Vickers microhardness (HV) tests and DSC measurements were carried out prior to the TEM experiments, to confirm the effect of heat treatments on the Vickers microhardness (HV) and the phase decomposition of the alloy specimen used in this study. Fig. 1 shows the HV curve of the Al–0.83Mg–0.4Si alloy aged at 483 K for aging times up to 60 ks. The HV hardness initially increased slowly with the aging time up to 1 ks, then increased more quickly. The hardness attained a peak value after 12 ks, then decreased due to overaging. These hardness tests therefore show that the Al–Mg–Si specimens reach the peak condition of hardness after annealing at 483 K for 12 ks, and specimens aged at this condition are suitable for TEM observation of metastable precipitates.

Fig. 2 shows DSC curves obtained for specimens aged isothermally at 483 K for various times up to 12 ks. The horizontal and vertical axes correspond to temperature and heat respectively. An exothermic peak, which is found above the base line, indicates the formation of second-phase precipitates or clusters. An endothermic peak, which corresponds to the dissolution of a phase, appears below the base line at a temperature range higher than the corresponding exothermic peak. The DSC curves in Fig. 2 show four exothermic peaks, K, P, Q and S, which are assigned to the formation of solute clusters, β″, β′ and βprecipitates respectively, based on previous studies [19]. The exothermic peak P, corresponding to the formation of β″precipitates, clearly decreases with prior aging time. This decrease corresponds to precipitation which occurred during the aging prior to these DSC measurements [14]. It can be noted that the exothermic peak P due to precipitation of β″shows an explicit decrease on isothermal annealing, which is different from those for other exothermic peaks. The series of DSC measurements suggests that two meta-stable phases β″ and β′, corresponding to peaks P and Q, respectively, have different thermal stabilities at 483 K, although the exothermic peaks of the phases appear closely in the DSC curves.

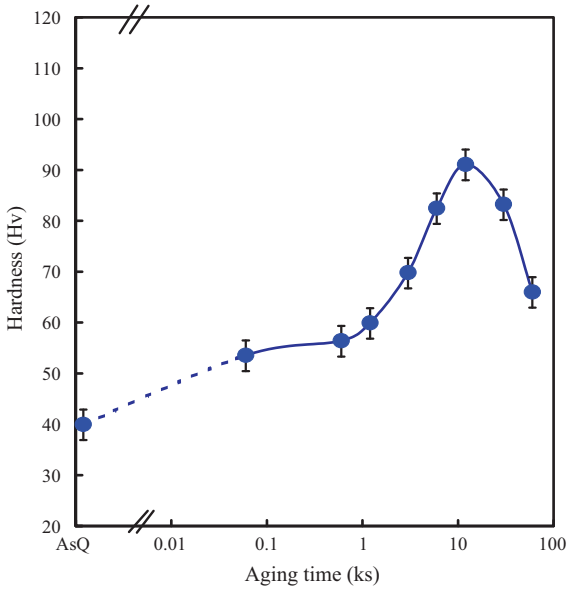

Fig. 1. Vickers microhardness curves of the Al–0.83Mg–0.4Si alloy aged at 483 K.

3.2. TEM observations and EDX analyses

Fig. 3 shows a bright-field TEM image of an Al–0.83Mg–0.4Si specimen aged at 483 K for 12 ks (at peak hardness). The incident beam was set parallel to the [0 0 1] direction of the Al matrix. This image shows that typical needle-shaped precipitates with lengths of 30–100 nm are formed, and lie along the [1 0 0] and [0 1 0] directions of the matrix. Granular particles 4–10 nm in diameter also

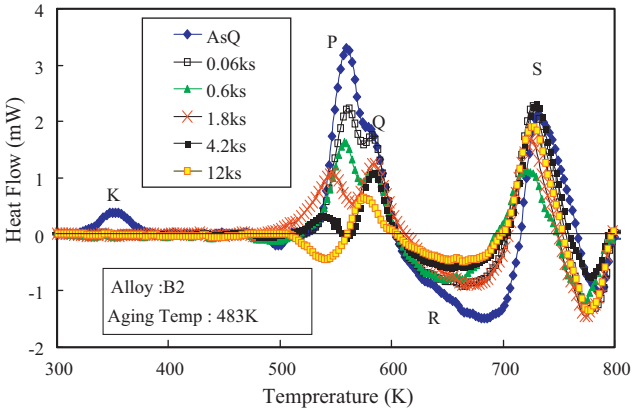

Fig. 2. DSC curves obtained for Al–0.83Mg–0.4Si specimens aged at 483 K.

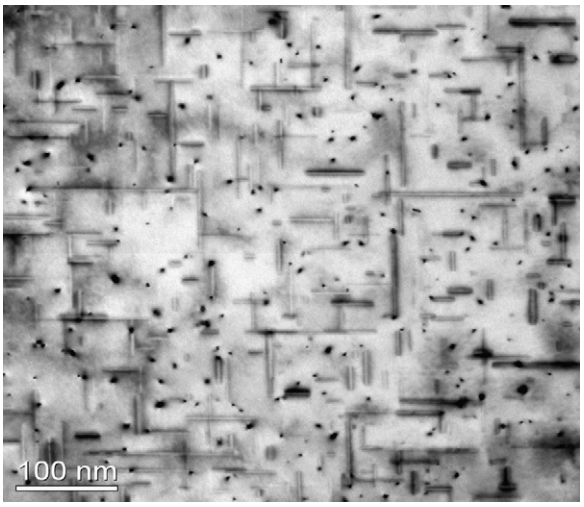

Fig. 3. A bright-field TEM image of an Al–0.83Mg–0.4Si specimen aged at 483 K for 12 ks (peak condition of HV hardness).

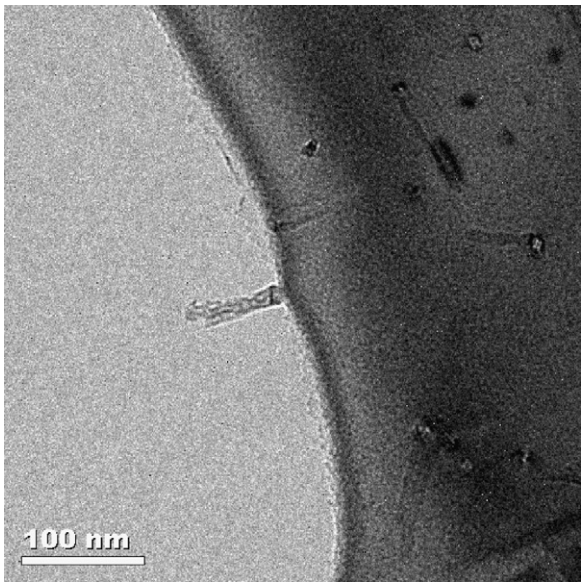

Fig. 4. A TEM image of a needle-shaped precipitate protruding from the edge of the hole in an electro-polished Al–Mg–Si specimen.

appear, but our tomography study confirmed that most of these were cross-sectional images of needle-shaped precipitates lying along [0 0 1], as previously mentioned.

Although EDX spectroscopy is recognized as an effective technique for determining the atomic composition of the precipitates formed in Al–Mg–Si alloys, the results reported in the literature have not fully been consistent. Some previous papers have claimed the presence of an Al peak in the energy spectrum, but others have insisted that no Al was contained in the precipitates. Analytical TEM-EDX examinations often face several significant problems; minimal limit of the electron probe size, low efficiencies for collecting X-ray signals of light elements, spectrum overlap effects, beam-induced contamination, and so forth. Smearing of the spectrum data can be also introduced by specimen drift during data acquisition, especially in the case that a small precipitate in the Al matrix is being analyzed. Furthermore, when the electron beam is incident on a needle-like precipitate lying parallel to the foil surface, the beam travels in the Al matrix surrounding the precipitate, resulting in a nominal increase of Al concentration. Thus in many cases, EDX point-analysis experiments could not rule out that Al peaks in the X-ray spectrum were largely or entirely due to the Al matrix.

Such difficulties remain even in recent EDX experiments. However, EDX mapping analysis with a modern FE-STEM instrument effectively shortens the acquisition time and to a large extent reduces the ambiguity of the EDX results. In addition to the use of FE-STEM and EDX, we have also examined in this work precipitates which protrude from the specimen edges. Examination of such precipitates allows us more confidently to eliminate the influence of the Al matrix. The number of precipitates protruding out at the edge of electro-polished specimens was small, but some were found.

Fig. 4 shows a TEM image of a needle-shaped precipitate protruding from the edge of the hole in an electro-polished specimen. The size of the precipitate is similar to those found inside the Al matrix. The TEM image also confirms that the direction of the rod coincides with a ⟨1 0 0⟩ direction of the matrix. It seems therefore that such precipitates are typical of those found within the specimen. Fig. 5 shows a STEM DF image of another needle-shaped precipitate projecting from the edge, together with the EDX spectrum of this precipitate and elemental maps obtained with the

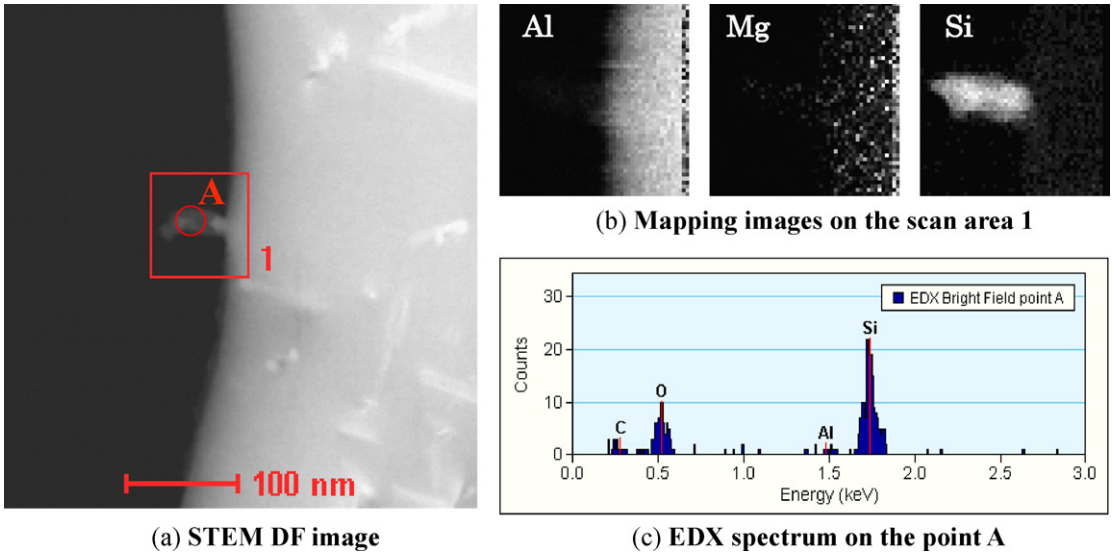

(a) **STEM DF image**

(b) **Mapping images on the scan area 1**

(c) **EDX spectrum on the point A**

Fig. 5. (a) A STEM DF image and (b) element maps obtained with characteristic X-rays of Al, Mg and Si, of a precipitate protruding from the specimen edge, together with (c) the EDX spectrum at the position A.

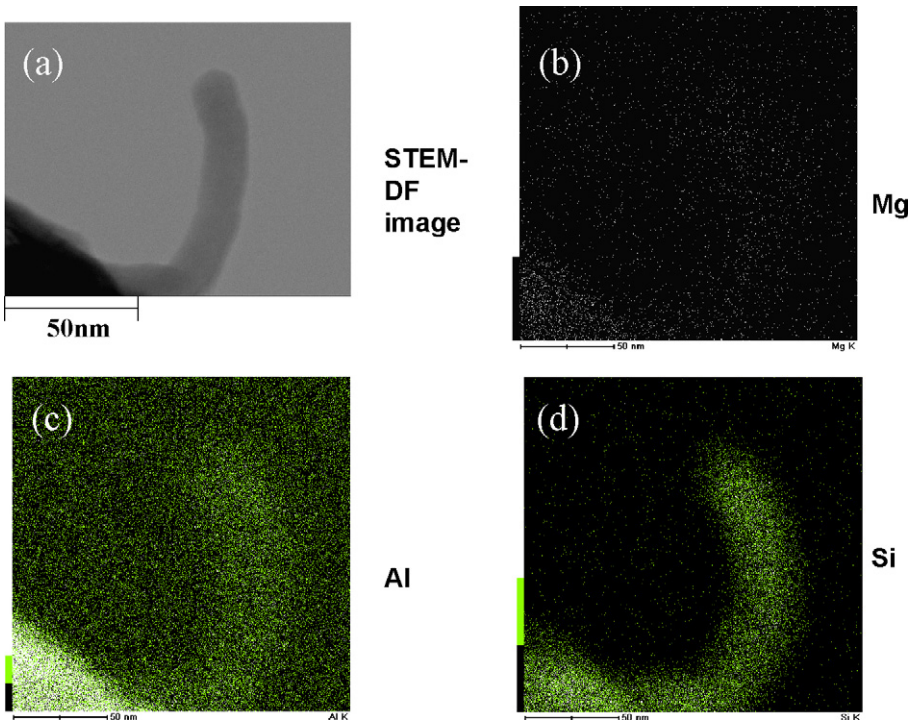

Fig. 6. (a) A dark-field STEM image of a small precipitate protruding from the edge of an electro-polished specimen and (b–d) corresponding STEM-EDX elemental-mapping images.

characteristic X-rays of Al, Mg and Si. The EDX spectrum shown in Fig. 5 (c) is almost free from the influence of the matrix and is dominated by the characteristic X-ray signal of SiKα with only a small contribution from AlKα. This clearly shows that the precipitates consist mainly of Si and that any Al or Mg is present only in very small amounts. The elemental maps shown in Fig. 5 (b) reinforce this conclusion. Sometimes we found protruding precipitates to be bent. The deformation of precipitates is probably caused by the flow of the electrolyte solution in jet-thinning. Such a bent precipitate is shown in Fig. 6, together with the EDX elemental maps. Again, the EDX elemental maps indicate that the precipitate comprises mostly Si with trivial amounts of other elements. These findings

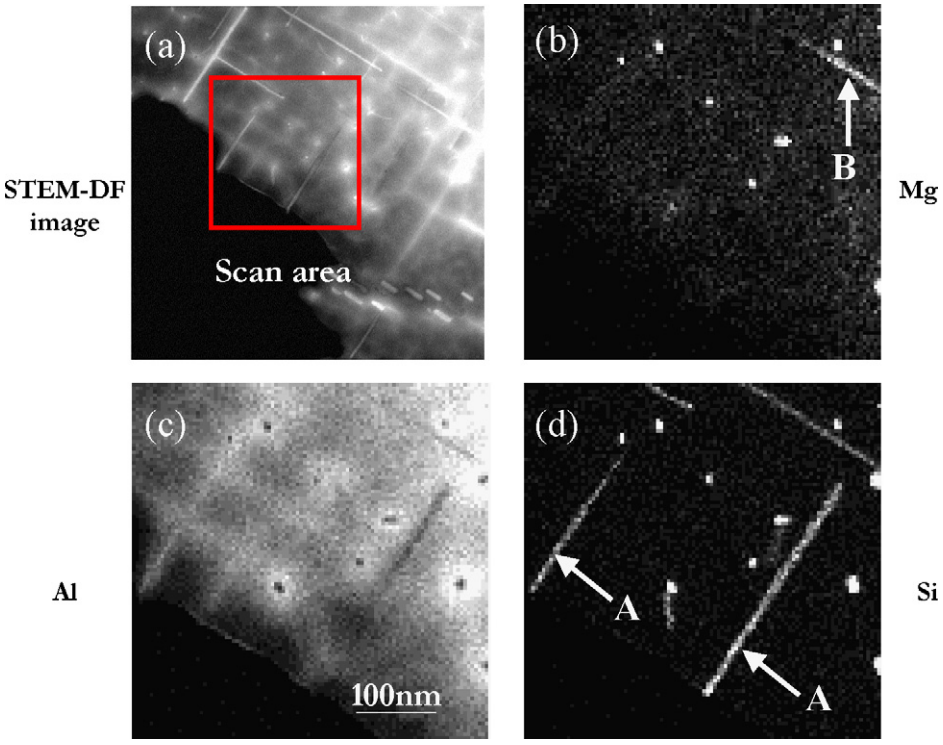

Fig. 7. (a) A dark-field STEM image of the examined area and (b–d) the corresponding STEM-EDX elemental-maps of precipitates within the bulk.

evidently show the necessity to scrutinize whether only one type of precipitate is formed, or if other types of precipitate coexist in this alloy.

To investigate this point, we applied STEM-EDX elemental-mapping to precipitates formed within the specimen. Fig. 7(a) shows a dark-field STEM image of the area examined and Fig. 7(b)–(d) shows corresponding STEM-EDX elemental-maps. Comparing the Mg and Si maps shown in Fig. 7 (b)–(d), respectively, we notice a striking feature: two types of needle-shaped precipitates with different compositions are formed simultaneously at the peak condition of hardness. Some appear to contain only Si (arrow A) while others of similar appearance contain both Mg and Si (arrow B). Thus, the present EDX experiment have revealed the following significant features of the precipitates at the peak aging condition: (1) needle-shaped Si-rich precipitates are formed, containing trivial amounts of Mg; (2) Mg–Si complex precipitates of similar appearance but perhaps of somewhat smaller size are also present; and (3) both types of precipitates contain relatively low quantities of Al.

To make a quantitative estimation of the composition of the precipitates, EDX point analysis was again carried out. The averaged value of the Mg:Si ratio in precipitates containing Mg was 0.87. Although this value is comparable to those previously reported [5,6], it should be noted that individual values of the Mg:Si ratio were distributed in a range 0.027–2.33. The Mg element map shown in Fig. 7 seems to reflect this, with some precipitates appearing more strongly than others.

Taking into account the Gibbs phase rule in thermodynamics, the supersaturated phase in an Al–Mg–Si ternary alloy may be decomposed into three phases. A quasi-equilibrium balance among these three phases possibly occurs below the eutectic temperature in the Al–0.83Mg–0.4Si (at%) alloy, if the three-phase region of $Al + Si + Mg_2Si$ slightly shifts from that formed at the eutectic temperature and extends to higher Mg content region at lower temperatures. In this case, metastable/stable Si-rich and Mg–Si phases can appear simultaneously in the alloy.

The present study has revealed that both Si-rich and Mg–Si precipitates form at the peak condition of hardness. This result is consistent with the DSC examinations [7,8,13–15]. As pointed out above, the experimental data on the composition of β″precipitates were scattered. The dispersion of data reflects real differences in the composition of individual precipitates, and this feature seems to be a part of the reason that different estimations have been reported on the composition of the precipitates in previous works. The precipitation sequence of solute clusters and metastable precipitates has not yet been completely elucidated. Precipitation is a phenomenon based on a diffusion process, and to understand the process consideration is also needed from this point of view. Further study to clarify and understand precipitation processes in Al–Mg–Si alloys is intended by the present authors.

4. Conclusions

The present work has investigated metastable precipitates formed at the peak-hardness condition in an Al–0.83Mg–0.4Si alloy (at%) aged isothermally at 483 K by means of Vickers microhardness tests, DSC measurements, FE-STEM and EDX elemental-mapping. The point-analysis and elemental maps obtained from EDX spectroscopy revealed that two types of precipitates consisting of Si and Mg–Si precipitates simultaneously. The average composition of the Mg–Si precipitates was Mg:Si = 0.87, although the estimated values of the ratio were distributed in the range 0.027 to 2.33. A combination of DSC measurements and TEM and EDX examinations suggest that needle-shaped Si-rich β″ precipitates were formed after clustering occurring around at 313–370 K, but prior to needle-shaped β′ precipitates.

Acknowledgment

The present authors sincerely thank to Dr. H.Yoshida, Sumitomo Light Metals Co., for providing Al–Mg–Si materials used in this study. The authors are also grateful to Dr. M. L. Jenkins, University of Oxford for critical reading and valuable discussions on the manuscript.

References

[1] G. Thomas, J. Inst. Met. 90 (1961–1962) 57.
[2] Jacobs, Phil. Mag. 26 (1972) 1.
[3] R.P. Wahi, m. Von Heimendahl, Phys. Stat. Sol. (a) 24 (1974) 607.
[4] J.P Lynch, L.M. Brown, M.H. Jacobs, Acta Metall. 30 (1982) 1389.
[5] G.A. Edwards, K. Stiller, G.L. Dunlop, M.J. Couper, Acta Mater. 46 (1998) 3893.
[6] M. Murayama, K. Hono, Acta Mater. 47 (1999) 1537.
[7] M. Takeda, F. Ohkubo, T. Shirai, J. Mater. Sci. 33 (1998) 2385.
[8] M. Takeda, K. Kurumizawa, S. Sumen, K. Fukui, T. Endo, Z. fuer Metallkde 93 (2002) 6.
[9] H.W. Zandbergen, S.J. Andersen, J. Jansen, Science 277 (1997) 1221.
[10] S.J. Andersen, H.W. Zandergen, J. Jansen, C. TrÆholt, U. Tundal, O. Reiso, Acta Mater. 46 (1998) 3283.
[11] S. Ramachandran, K. Jung, J. Narayan, H. Conrad, Mater. Sci. Eng. A 435–436 (2006) 693.
[12] K. Matsuda, S. Tada, S. Ikeno, T. Sato, A. Kamio, Scripta Mater. 32 (1995) 1175.
[13] K. Fukui, M. Takeda, T. Endo, Mater. Sci. Forum 475–479 (2005) 365.
[14] K. Fukui, M. Takeda, T. Endo, Mater. Lett. 59 (2005) 1444.
[15] K. Fukui, M. Takeda, T. Endo, Mater. Trans. 46 (2005) 880.
[16] J.R. Kremer, D.N. Mastronarde, J.R. McIntosh, J. Struct. Biol. 116 (1996) 71.
[17] K. Kaneko, W.J. Moon, K. Inoke, Z. Horita, S. Ohara, T. Adschiri, H. Abe, M. Naito, Mater. Sci. Eng. A403 (2005) 32.
[18] S.K. Son, S. Matsumura, M. Takeda, K. Fukui, Proc. Int. Micros Conf. (2006).
[19] I. Dutta, S.M. Allen, J. Mater. Sci. Lett. 10 (1991) 323.